

Removal of Congo Red from Aqueous Solution Using Cuttlefish Bone Powder

H. Yazid^a, Y. Achour^{a,b,*}, A. El Kassimi^a, I. Nadir^a, M. El Himri^a, M.R. Laamari^a and M. El Haddad^{a,*}

^aLaboratoire de Chimie Analytique et Moléculaire, Faculté Poly-disciplinaire, Université Cadi Ayyad, BP 4162, 46000 Safi, Maroc

^bLaboratoire de Chimie Organique et Analytique, Faculté des Sciences et Techniques, Université Sultan Moulay Slimane, BP 523, 23000 Beni-Mellal, Maroc

(Received 2 April 2021, Accepted 10 June 2021)

Adsorption experiments were carried out as a part of the removal of Congo red (CR), a textile dye, from aqueous solutions using the powder of cuttlefish bone (*Sepia*) as a new potential adsorbent. The prepared powder was characterized by FTIR, XRD, SEM and elemental analysis. The effects of solution pH, adsorbent amount, CR concentration, temperature and contact time on the CR adsorption were investigated. The experimental results showed that maximum pH was about 2 for efficient uptake of CR. The equilibrium was attained in 60 min. The adsorption of Congo red was found to be exothermic in nature ($\Delta H^\circ = 8.41 \text{ kJ mol}^{-1}$), while the positive value of entropy $20.85 \text{ J mol}^{-1} \text{ K}^{-1}$ indicated an increased randomness at the solid/liquid interface. The experimental data were analyzed using Langmuir and Freundlich isothermal models. The best fit was obtained by Langmuir model with a maximum monolayer adsorption capacity of 69.9 mg g^{-1} . Adsorption kinetics data were properly fitted with the pseudo second-order kinetic model.

Keywords: Cuttlefish bone, Congo red, Removal dye, Kinetic, Isotherms

INTRODUCTION

The elimination of dyes from textile industry effluents is one of the most important environmental problems in the framework of environmental protection [1]. Dyes are widely used in modern industrial units [2]. Due to their synthetic origin and their complex aromatic molecular structures, which make them inert and not easy to biodegrade when discharged into the environment system [3], generally, people overlook their undesirable nature. Some dyes are harmful to aquatic life where they are discharged as well as to human life [4].

Permanent exposure in the industrial environment of workers in the textile industries is linked to a higher risk of different types of cancer [5]. The use of hair coloring products is one of the causes of breast cancer [6]. Therefore, several documents and research programs have been

developed using different methods to remove dye species from wastewater. There are several varieties of dyes due to their structures, such as acid, basic, azo, diazo, disperse, anthraquinone and metal complex dyes. Currently known treatment methods can be physical, chemical and biological in nature [7], namely adsorption [8], advanced oxidation processes [9], coagulation and flocculation [10], ozonation [11], electroflotation [12], electrokinetic coagulation [13], membrane filtration [14], irradiation [15], electrochemical destruction [16], ion exchange [17], precipitation and biological treatment [18]. It should be noted that most of these processes have significant weaknesses, including partial elimination of dyes, the need to use high quantities of reagents and energy, poor selectivity, high capital and operating costs, and the production of secondary waste or high toxicity by-products that are difficult to eliminate or degrade [19]. However, the adsorption technique represents a powerful alternative for the removal of dyes as well as other pollutants including heavy metals contained in industrial wastewater [20]. In principle, adsorption is a

*Corresponding authors. E-mail: youness.achour@gmail.com; elhaddad71@gmail.com

process in which a solid adsorbent attracts a component in an aqueous solution to its surface and subsequently form a bond of a physical or chemical nature, to remove pollutants from liquid solutions. The use of low-cost adsorbents has proven to be an efficient and economical method of treating effluents by adsorption, which offers additional advantages over conventional processes, particularly from an environmental point of view [21]. However, the low cost and high adsorption capacity of adsorbents are still being studied and developed to reduce the amount of adsorbent and at the same time minimizing experimental problems in term of removal efficiency. A great deal of attention has recently been paid by various researchers using various adsorbent materials that are low cost, easy to obtain and biodegradable, namely animal bones [22] and shellfish waste [23], which can be collected in large quantities and are harmless to nature. Several adsorbent materials have been tested for their ability to remove dyes from aqueous solutions.

The present study highlights the adsorption of Congo red from aqueous solutions using cuttlebone powder (CFB) as a new ecological and potentially alternative adsorbent in terms of valuing this marine waste, with the aim of eliminating chemical pollutants as well as opening other perspectives. The adsorption process of Congo red has been studied to optimize experimental conditions for the best adsorption of CR, such as the effect of the amount of adsorbent, initial dye concentration, contact time, pH and temperature. The study describes the adsorption equilibrium of Congo red and the presentation of kinetic and isothermal models of the experimental data, which collaborated with its thermodynamic properties. Finally, the new adsorbent was characterized by FT-IR, SEM, DRX and elemental analysis of the powder.

MATERIALS AND METHODS

Reagents

Congo red was purchased from Sigma-Aldrich (Molecular Weight: 696.66 g/mol; molecular formula of $C_{32}H_{22}N_6Na_2O_6S_2$; Color Index Number: 22120) with high quality. NaOH and HCl were used to adjust the pH of aqueous solutions. The preparation of 100 mg l⁻¹ of the stock solution was carried out by dissolving a known

amount of CR in a 1000 ml volumetric flask and then diluting with bi-distilled water for the further use.

Equipments

The adsorption procedure was performed using a multiple magnetic stirrer (MIXdrive 15, Germany). A UV-Vis spectrophotometer (JENWAY 6300) and a pH meter (HANA HI 4222) were used to determine the dye concentration during the adsorption process and pH adjustment of aqueous solutions, respectively. The surface morphology was analyzed through a scanning electron microscope (TESCAN VEGA 3) at high voltage 20 kV. FT-IR spectra (4000-400 cm⁻¹ range) were recorded by a VERTEX 70 FT-IR. The XRD analysis was performed at laboratory temperature using a Rigaku SmartLab diffractometer (copper anode [$K\alpha = 1.5418\text{\AA}$]). The diffractograms were recorded in the range ($2\theta = 5-90^\circ$) with a step size of 0.02°.

Adsorbent Preparation

Cuttlefish bone (Sepia), a sea product available in seaside areas, was collected from the Safi Sea. Before being used, the bones were washed several times with bi-distilled water, dried at 103-105° for 24 h and then left to cool in a desiccator. These bones were ground and reduced to a fine powder using a planetary mill equipped with ZrO₂ balls. Finally, the product was stored in a glass bottle.

Adsorption Process

The adsorption of Congo red was carried out in a batch process using the new prepared Cuttlefish bone (CFB). For this reason, a known amount of CFB was added to a 50 ml volume of dye solution (containing 40 mg l⁻¹ CR). The pH of the dye solution was adjusted with 0.1 M HCl and NaOH solution. The mixture was then stirred magnetically at 20 °C for 60 min. After centrifugation, the supernatant solution containing the unadsorbed dye was introduced into the UV-Vis spectrophotometer to measure the actual concentration of CR remaining in the supernatant. The amount of adsorbed dye at equilibrium q_e (mg g⁻¹) was calculated through the following relation:

$$q_e = \frac{C_0 - C_e}{W} V \quad (1)$$

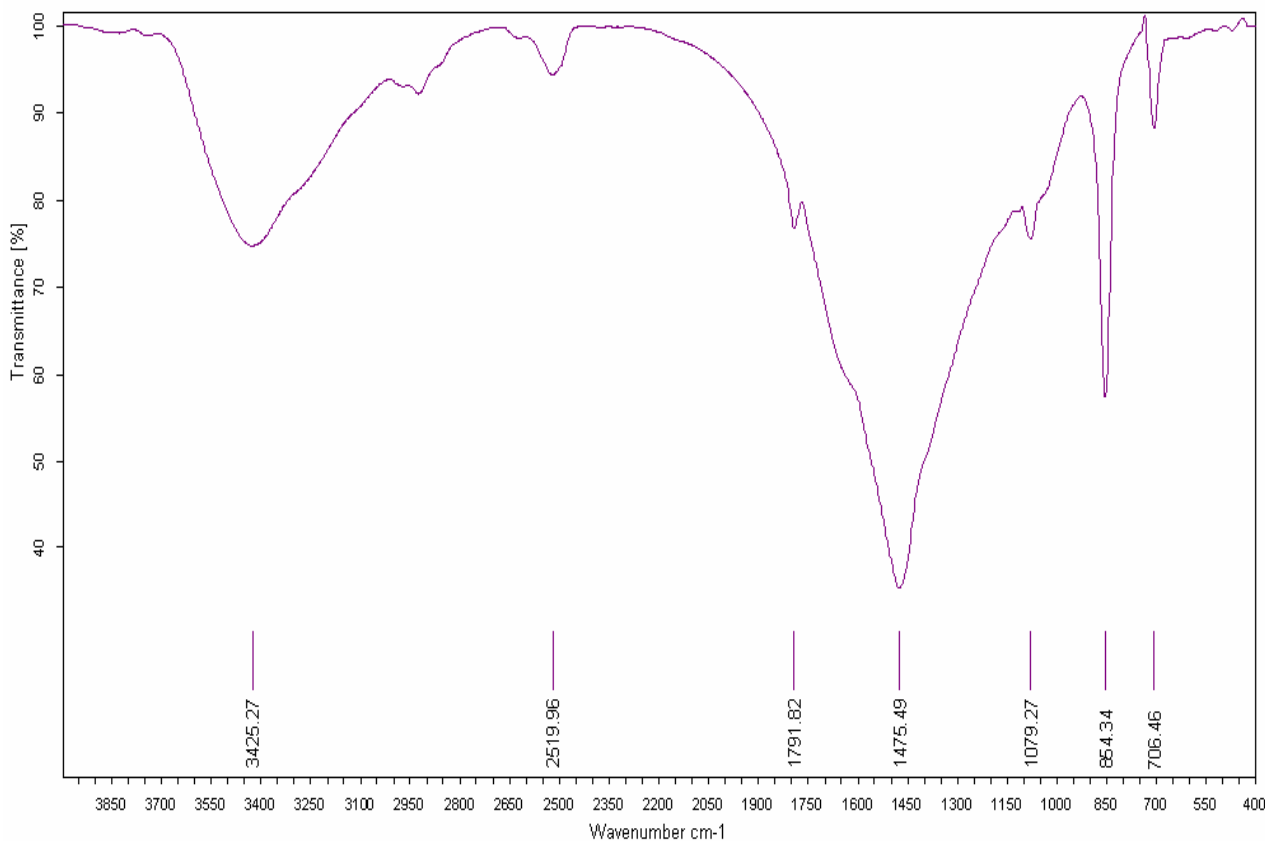


Fig. 1. FTIR spectrum of CFB.

C_e and C_0 are the concentration of dye remained in solution at equilibrium and the initial concentration of dye solution, respectively. V is the volume of the dye solution and W is the mass of the adsorbent used.

The removal efficiency was calculated using the following equation:

$$\% \text{Adsorption} = \frac{C_0 - C_e}{C_0} \times 100 \quad (2)$$

C_0 and C_e are the initial dye concentration and the concentration at equilibrium, their unit is mg l^{-1} .

RESULTS AND DISCUSSION

Characterization of Cuttlefish Bone (Sepia)

Figure 1 shows the FTIR spectra for CFB as follows: A

wide band at 3425 cm^{-1} has been assigned to the O-H stretching vibration mode of the hydroxyl functional group. Peaks in the range of 2519 cm^{-1} indicate the presence of $-\text{NH}_2$ stretching. A wideband at 1475 cm^{-1} was attributed to C-O, 1079 cm^{-1} corresponding to $-\text{C}-\text{NH}_2$, and the bands at wave numbers 854 and 706 cm^{-1} were assigned to $\text{CH}_2=\text{C}-$ and $-\text{CH}=\text{CH}$, respectively.

Examination of the textural structure of internal cuttlefish, and cuttlefish bone can be seen through the SEM images in Fig. 2. In Fig. 2b, the cuttlefish bone shows a very porous structure with a non-homogeneous and non-smooth surface that can easily adsorb dye molecules. The elemental analysis were done by EDAX (Fig. 3) which reveals the presence of elements like C, O, Fe and a high content of Ca.

As shown in Fig. 4, the X-ray diffraction pattern (XRD) shows that CFB has a well-crystallized shape with a low

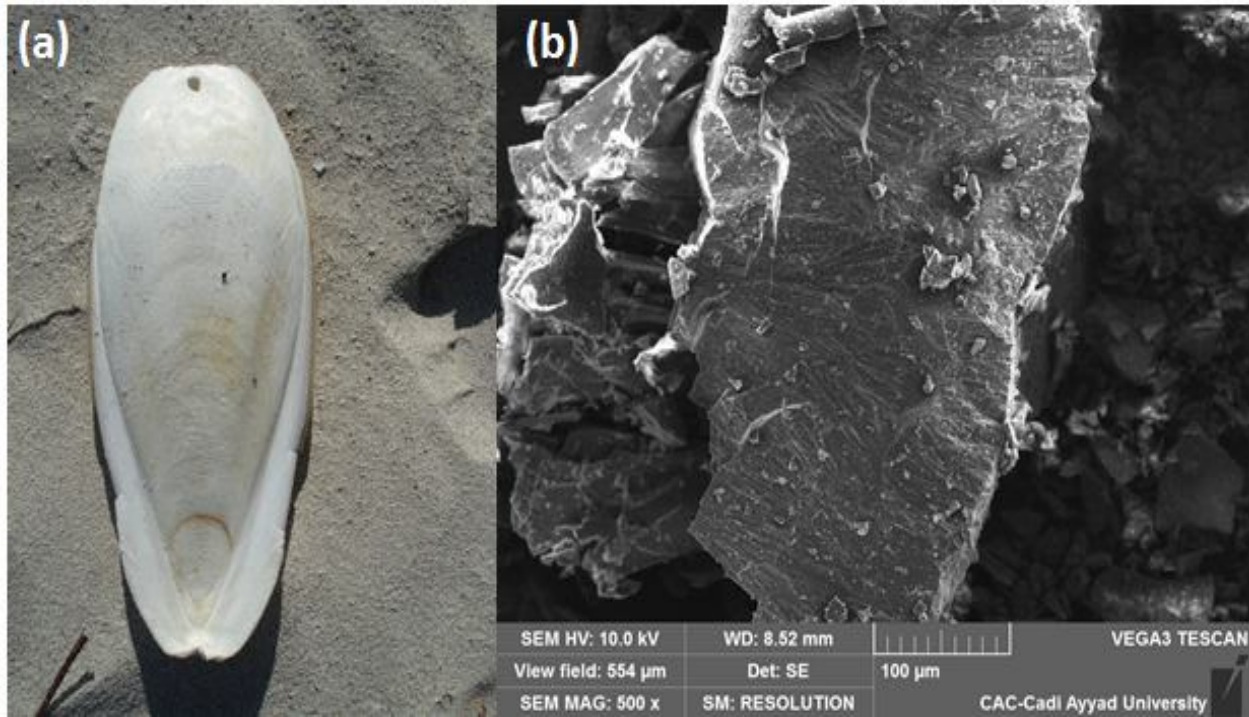


Fig. 2. Internal cuttlefish (a) and SEM image of CFB (b).

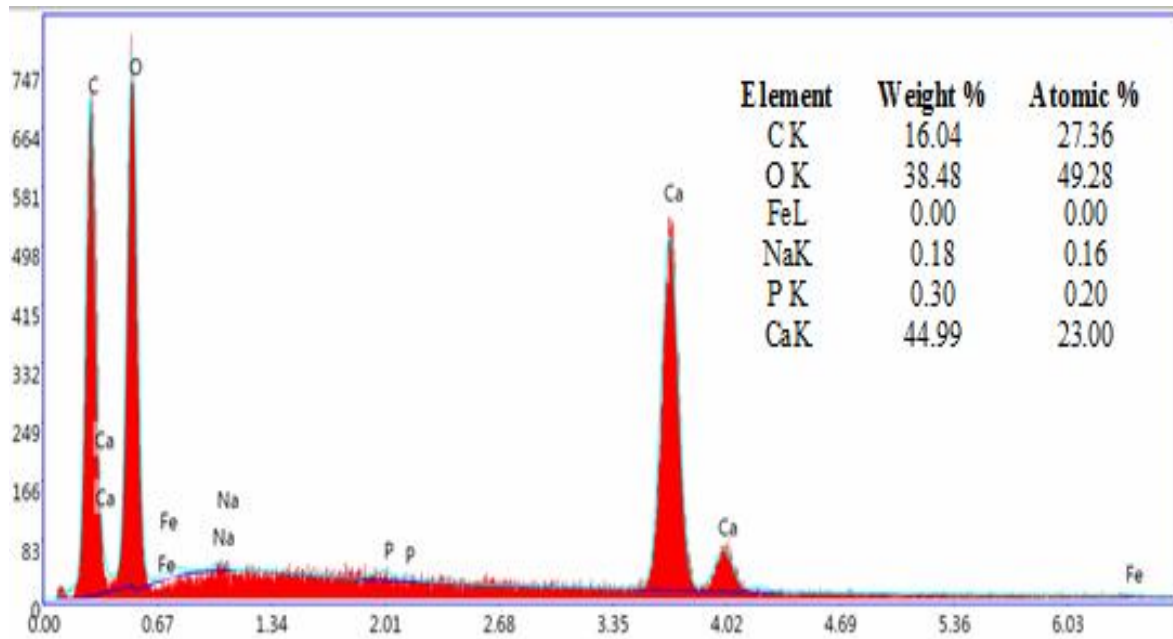


Fig. 3. EDX spectra of CFB.

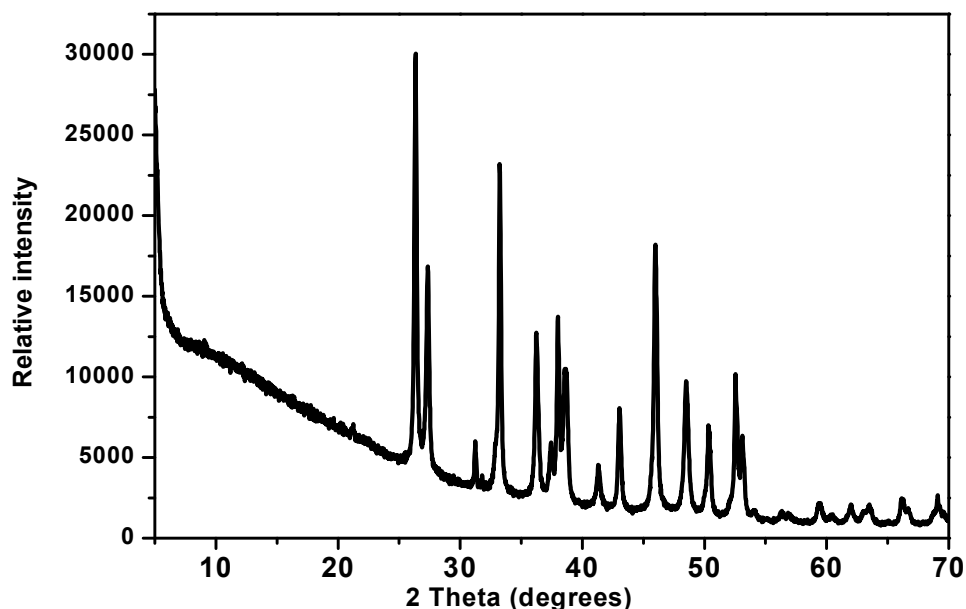


Fig. 4. XRD pattern of cuttlefish bones.

peak at 27° , which is representative of the aragonite variety. Besides, the numerous CaCO_3 peaks on the right side of the spectrum are moderately dominant, indicating the presence of a CaCO_3 .

Effect of Adsorbent Ddose

The effect of the CFB dosage on the uptake (mg g^{-1}) is shown in Fig. 5. The adsorbent dosage was varied from 50 to 150 mg using $V = 50$ ml of CR (100 mg l^{-1}) at room temperature. Adsorption capacities increase with time and the response becomes constant for all quantities studied beyond 60 min. Maximum absorption ($q_e = 23.71 \text{ mg g}^{-1}$) was observed with the 50 mg dose. The adsorption capacity decreased slightly while increasing the adsorbent dose. This may be due to inter-particle interactions, namely the aggregation, a result of an increase in the adsorbent dose. Aggregation may refer to a decrease in the total surface area of the adsorbent and certainly an increase in the length of the diffusion path [24,25].

Effect of Initial Dye Concentration and Contact Time

The effect of initial concentration of dye ranged from

($50\text{-}150 \text{ mg l}^{-1}$) at room temperature on CR removal was studied by adsorption onto CFB in different interval times (0-90 min). Figure 6 depicts these results. It was observed that the amount of adsorbed CR increases with the evolution of contact time in all initial dye concentrations. Furthermore, the adsorption capacity of CR increases with the increase of initial dye concentration. At a higher concentration, the ratio between the available surface area and the initial number of dye molecules is high; therefore, fractional adsorption becomes dependent on the initial concentration. Otherwise, at low concentrations, fewer adsorption sites are available and the amount of CR adsorbed depends on the concentration. Based on these results, it appears that during the first 60 min, the amount of adsorbed CR was rapid, then it continues at a slower rate of adsorption and finally reaches saturation within 60 min [26,27].

Effect of pH on the Removal of CR on to Cuttlefish Bone

It is recognized that the pH of the solution remarkably affects the adsorption capacity of the dye using adsorbents, since hydrogen ions affect the surface charge of the

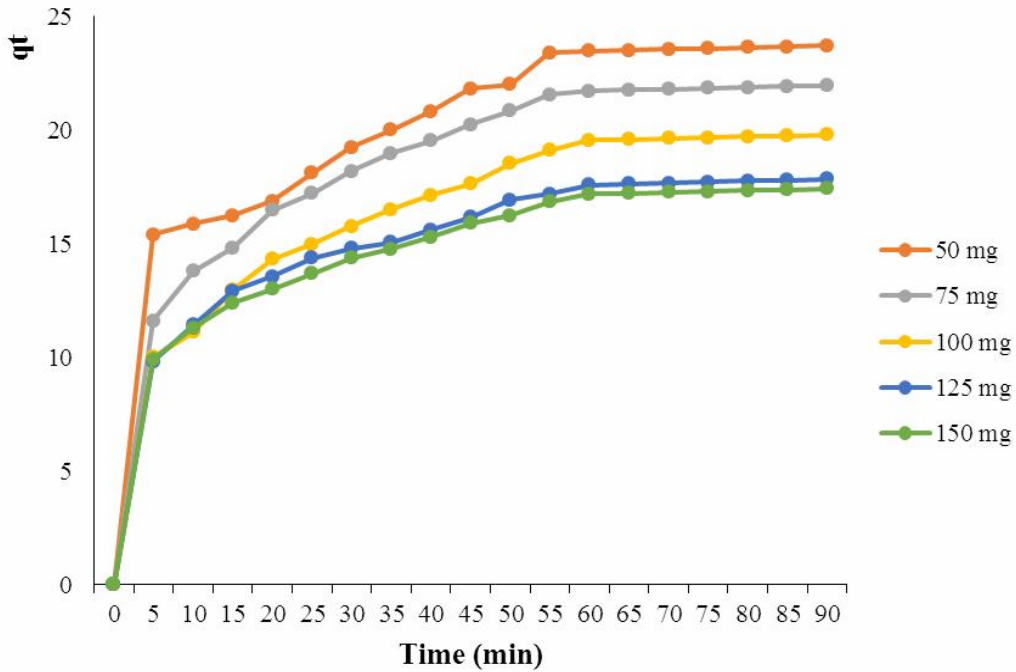


Fig. 5. Effect of CFB dose on the removal of CR: [CR] = 100 mg l⁻¹, V = 50 ml and T = 20 °C.

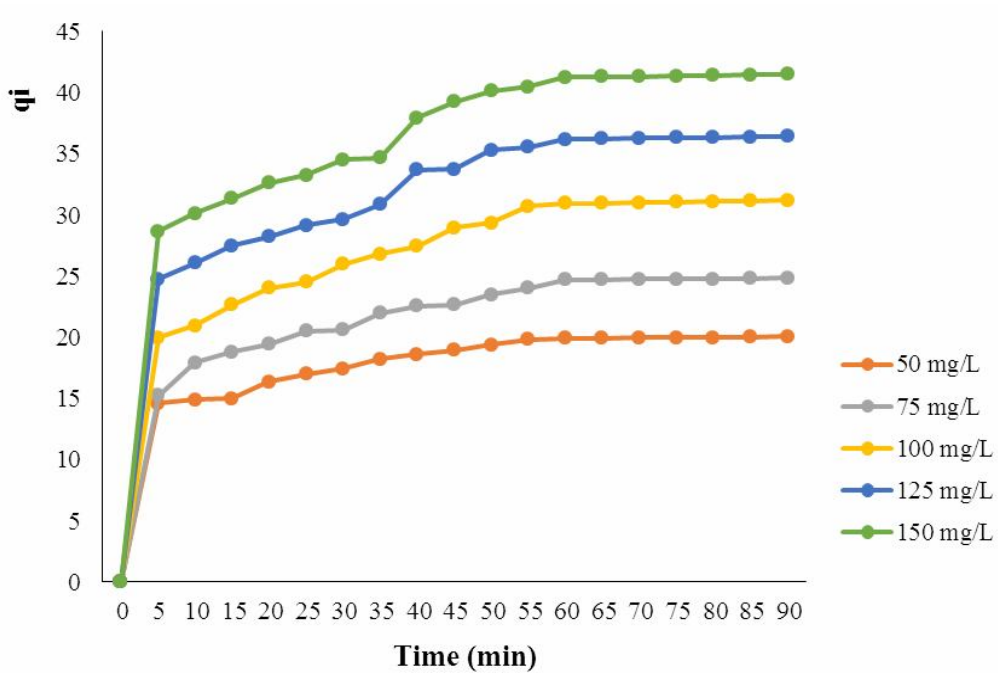


Fig. 6. Effect of initial concentration and contact time on the removal of CR from aqueous solution: [CB] = 75 mg; V = 50 ml and T = 20 °C.

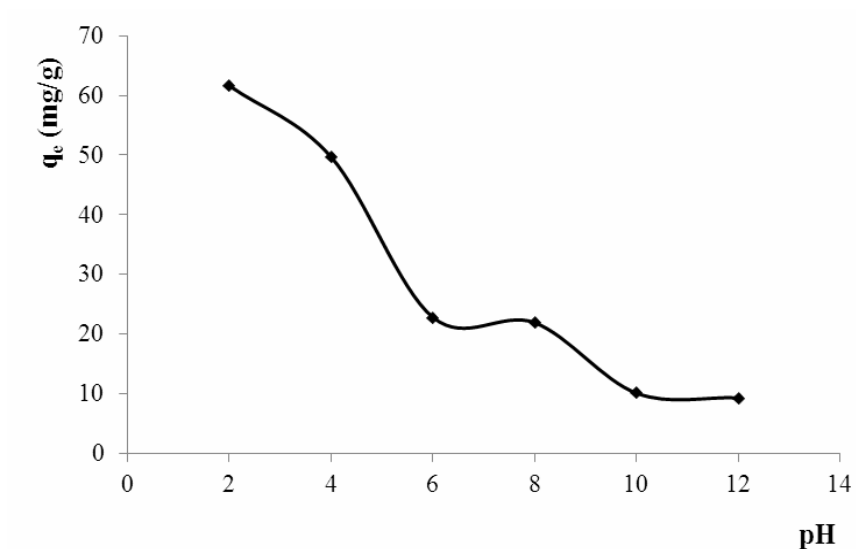


Fig. 7. Effect of initial pH on the removal of CR from aqueous solution: [CR] = 100 mg l⁻¹; V = 50 ml and T = 20 °C.

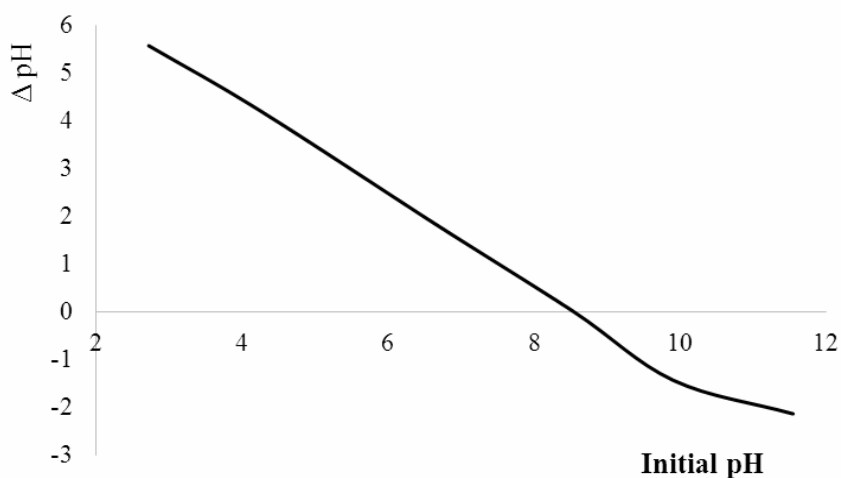


Fig. 8. Determination of zero point charge pH.

adsorbent [28,29]. In order to study the effect of pH on the absorption of CR by the CFB adsorbent, we determined the adsorption capacity as a function of pH in a range of 2-12. The results of this investigation is given in Fig. 7. The calculated pH zero point charge (pH_{ZPC}) was found to be 8.5 as shown in Fig. 8. The pH_{ZPC} of CFB shows that the adsorbent surface is positively charged at pH values below 8.5 and negatively charged at pH values above 8.5. Congo

red absorption decreases from 61.6 to 9.3 mg g⁻¹ when the pH decreases from 2 to 12. At a lower pH, the overall surface charge of CFB is positive, which will promote adsorption interactions with Congo red as an anionic dye by the electrostatic attractive forces that could be the main mechanism for adsorption of Congo red molecules to the surface of CFB. Namely, since Congo red species carry a negative charge due to the presence of sulfonate groups, the

electrostatic attractions should have an important contribution to the overall interactions [30,31].

Kinetics Study

Several models are used to explain the adsorption mechanism of dyes. The speed and the mechanism of adsorption of dyes are both controlled by various factors, namely the physical and chemical properties of the adsorbent and the mass transfer process. These kinetic models are intended for the design and optimization of the dye treatment process. In order to study the mechanism of CR adsorption by CFB, two kinetic models, pseudo-first-order and pseudo-second-order were considered. Lagrange proposed that the pseudo first-order model is used to test the fit of the experimental results obtained [32], and the model is presented by the following equation:

$$\log(q_e - q_t) = \log(q_e) - \frac{k_1}{2.303}t \quad (3)$$

where, q_e is the adsorbed amount of CR at equilibrium (mg g^{-1}), q_t is the adsorbed amount of CR at a known time t (mg g^{-1}), k_1 is the rate constant of the first-order model (min^{-1}) and t is time (min). A linear fit is expected by plotting $\log(q_e - q_t)$ as a function of t , provided that the adsorption process follows first-order kinetics by adjusting the equilibrium data. The values of k_1 and q_e are calculated from the slope and intercept of the model equation. The results of the logarithmic curve ($q_e - q_t$) vs. time at initial CR concentrations (50 to 150 mg l^{-1}) are presented in Table 1. The calculated values of the equilibrium adsorption capacities q_e (cal) and q_e (exp) clearly showed an important difference between these two capacities. The pseudo-first-order model failed to fit the experimental data of CR adsorption onto CFB.

The pseudo-second-order kinetic model is also used to describe the adsorption process [33], in case the first-order kinetic model does not fit well with the experimental data. The pseudo-second-order model is presented through the following equation:

$$\frac{t}{q_t} = \frac{1}{k_2 q_e^2} + \frac{1}{q_e}t \quad (4)$$

where k_2 is the pseudo-second-order rate constant

($\text{g mg}^{-1} \text{min}^{-1}$). The plot of (t/q_t) in function of (t) should give a linear curve if the model fits the experimental data. The values of q_e and k_2 are calculated from the slope and intercept of the linear curve. The results are gathered in Table 1.

The values of the equilibrium adsorption capacity q_e (cal) and q_e (exp) are in close agreement with a small difference between these capacities for all the studied concentrations. The linear curves of (t/q_t) as a function of (t) in different concentrations of CR are fitted in Fig. 9. The experimental data for the adsorption of CR by CFB are well fitted by the pseudo-second order kinetic model with very high R^2 coefficients as well as the CR adsorption rate; chemical adsorption is specific and involves much stronger forces (chemical bonds) than physical adsorption. Thus, the activation energy of chemical adsorption is of the same order of magnitude as the heat of chemical reactions, meaning that the rate varies with temperature as a function of finite activation energy. This indicates that the adsorption phenomenon could be chemisorption in nature [34,35].

Adsorption Isotherm

Isothermal equilibrium models are used to process and describe experimental CR adsorption data, with relative parameters obtained from the different established models (Table 2). The equilibrium data of the CR adsorption process were analyzed using Langmuir and Freundlich isothermal models. Linear regression is used to determine the most appropriate model and compares the models by judging the R^2 correlation coefficient. The Langmuir isotherm is notionally based on the assumption that the adsorption energy is constant and independent of the coverage of the adsorbent surface where adsorption occurs at localized sites without interaction between the molecules of the pollutant, the model equation is given as follows [36]:

$$\frac{C_e}{q_e} = \frac{1}{q_m K_L} + \frac{C_e}{q_m} \quad (5)$$

where q_e (mg g^{-1}) is the adsorbed amount of CR at the equilibrium stage, C_e (mg l^{-1}) is the concentration of CR at equilibrium. q_{max} (mg g^{-1}) and K_L (l mg^{-1}) are Langmuir model constants related to adsorption capacity and adsorption rate, respectively. A straight curve with a slope

Table 1. Kinetic Data for Congo Red Removal

Concentration	Pseudo-first-order			Pseudo-second-order			
	k_1 (min^{-1}) $\times 10^{-2}$	$q_e(\text{cal})$	$q_e(\text{exp})$	R^2	k_2 ($\text{g mg}^{-1} \text{min}^{-1}$) $\times 10^{-4}$	$q_e(\text{cal})$	R^2
50	7.139	14.791	19.921	0.853	5.787	21.276	0.994
75	5.066	15.523	24.705	0.935	3.783	26.315	0.993
100	5.987	24.322	30.946	0.843	2.203	34.482	0.989
125	5.757	25.644	36.196	0.897	1.637	40	0.988
150	5.757	28.183	41.254	0.903	1.268	45.454	0.988

Table 2. Isotherm Data for CR Uptake

Temperature (K)	Langmuir			Freundlich		
	q_{max}	K_L	R^2	K_F	n	R^2
298	62.5	0.019	0.9973	4.27	2	0.9812
308	66.8	0.173	0.9951	6.02	1.29	0.9827
318	69.9	0.384	0.9929	12.94	1.13	0.9874

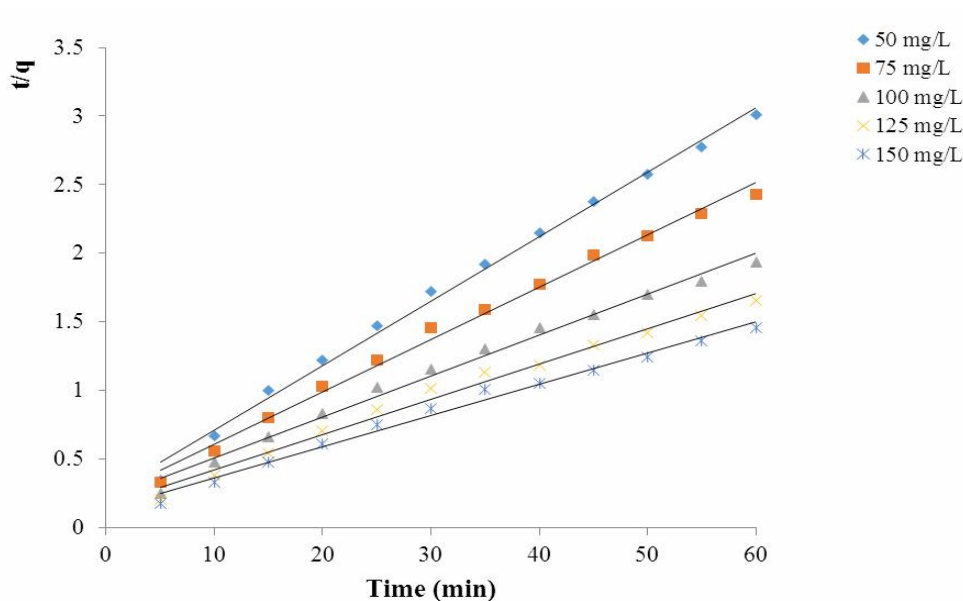


Fig. 9. Plot for the equation of pseudo-second-order model of CR.

of $(1/q_{max})$ and an intersection point of $(1/q_{max} K_L)$ is obtained when the ratio C_e/q_e is plotted as a function of C_e . The essential characteristics of the Langmuir equation can be expressed by calculating the dimensionless separation factor R_L obtained from the following equation:

$$R_L = \frac{1}{1 + K_L C_0} \quad (6)$$

where C_0 is the initial CR concentration. R_L is considered to be a reliable indicator of the adsorption phenomenon. There are four cases for R_L values:

- Unfavorable $R_L > 1$
- Linear $R_L = 1$
- Favorable $0 < R_L < 1$
- Irreversible $R_L = 0$

The linearized Langmuir isotherm explains well the experimental equilibrium data of CR adsorption over the studied temperature range of 298-318 K and the correlation coefficients are presented in Table 2. The values of q_{max} and K_L are also presented in Table 2. The correlation coefficients are high ($R^2 > 0.99$). The adsorption capacities of CR range from 62.5-69.9 mg g⁻¹, with a temperature range of 298-318 K. The results show that the R_L values are between 0 and 1 for the different temperatures, indicating that CFB is a suitable adsorbent for CR contained in aqueous solutions and the adsorption phenomenon is favorable. According to the results, the Langmuir isotherm fits well with the experimental data of the adsorption process of CR on CFB. This may be related to the homogeneous distribution of active sites on the surface of the CFB powder.

In addition, Freundlich's isothermal model is an equation based on the principle that adsorption takes place on a heterogeneous adsorbent surface or sites of various affinities [37]. The Freundlich isotherm is expressed through the following equation:

$$\log(q_e) = \log(K_f) + \frac{1}{n} \log(C_e) \quad (7)$$

where q_e (mg g⁻¹) is the adsorbed amount of CR on the CFB

at equilibrium stage, C_e (mg l⁻¹) is the concentration of CR in solution at equilibrium, n is the heterogeneity factor, and K_f (mg g⁻¹) (l g⁻¹)^{1/n} is the Freundlich constant related to the adsorption capacity. The constants K_f and $1/n$ of the Freundlich isotherm are obtained from the intercept and slope of the linear curve of $\log(q_e)$ versus $\log(C_e)$. The Freundlich constants are presented in Table 2. Values of n between 1 and 10 represent a favorable adsorption. By comparing the linear correlation coefficients of the two isotherms presented in Table 2, it can be concluded that the Langmuir isotherm fits well with that of the adsorption of CR on CFB in the selected temperature range. The adjustment of the experimental adsorption data to the Langmuir isotherm implies that the binding energy over the entire surface of the adsorbent is uniform. Finally, the adsorbed CR molecules form a monolayer on the surface of the CFB.

Effect of Temperature and Thermodynamic Functions

In order to test the ability of the removal efficiency of CR from aqueous solutions onto CFB, we conducted a temperature evaluation. Equilibrium data were collected at different temperatures: 298 K, 308 K, 318 K and 328 K. Some thermodynamic functions such as free energy change ΔG° , enthalpy ΔH° and entropy ΔS° were also used in order to describe the behavior of CR removal efficiency onto CFB and were calculated using the following equations:

$$K_0 = \frac{C_{solid}}{C_{liquid}} \quad (8)$$

$$\Delta G^\circ = -RT \ln K_0 \quad (9)$$

$$\ln K_0 = \frac{\Delta S^\circ}{2.303} R - \frac{\Delta H^\circ}{2.303} RT \quad (10)$$

where K_0 is the constant of equilibrium, C_{solid} (mg l⁻¹) is the concentration of CR in the solid phase at equilibrium, C_{liquid} (mg l⁻¹) is the concentration of CR in the liquid phase at equilibrium, T is the temperature in Kelvin, and R (8.314 J mol K⁻¹). Table 3 shows the values of ΔH° and ΔS° calculated from the slope and intercept of the Van't Hoff plot. The positive calculated value of ΔH° was found to be

Table 3. Thermodynamic Properties of CR Adsorption onto CFB

T (K°)	ΔG (kJ mol ⁻¹)	ΔH (kJ mol ⁻¹)	ΔS (kJ mol ⁻¹)
298	2.19920265	8.4154308	20.859826
308	1.99060439		
318	1.78200613		
328	1.57340787		

equal to 8.41 kJ mol⁻¹, which leads to conclude that the adsorption was endothermic. Additionally, the binding between the CR dye molecules and the surface of CFB is very weak [38]. The positive calculated values of ΔS° (20.85 J mol⁻¹ K⁻¹) (Table 3) indicate an increase in disorder with the randomness at the interface film of the solid solution of the dye with the CFB, resulting in some structural changes in the CFB and CR dye, also the irreversibility and stability of the biosorption process, and the affinity of CFB to CR. The increase in the adsorption capacity of CR with increasing temperatures has been probably attributed to enlarged pore size and possibly liquid penetration into the inner pores [39]. The decreased values of ΔG° from 2.19 to 1.57 kJ mol⁻¹ with the increase of the temperature from 298 to 328 K shows simultaneously an increase in feasibility of the adsorption phenomenon at high temperatures.

CONCLUSIONS

In this study, the powder of cuttlefish bone (*Sepia*) was investigated as a new low-cost and efficient adsorbent for the removal of CR dye from aqueous solutions. The prepared powder was characterized by FTIR, XRD, SEM and elemental analysis. The experimental factors such as CFB dose, contact time, Congo red concentrations, pH, adsorption kinetic, isotherm models and thermodynamic functions were investigated to study the adsorption phenomenon. The kinetics study of Congo red indicates that the adsorption phenomenon could be chemisorption in nature. The adsorption equilibrium data of CFB on CFB

was well adapted to the Langmuir isotherm and the adsorbed dye molecules formed a monolayer. With an increase in the temperature from 298 to 318 K, the increase in the adsorption capacity was obtained as 62.5 to 69.9 mg g⁻¹, respectively.

REFERENCES

- [1] Yagub, M. T.; Sen, T. K.; Afroze, S.; Ang, H. M., Dye and its removal from aqueous solution by adsorption: A review. *Adv. Colloid. Interface. Sci.* **2014**, *209*, 172-184, DOI: 10.1016/j.cis.2014.04.002.
- [2] Pavithra, K. G.; Kumar, P. S.; Jaikumar, V.; Rajan, P. S., Removal of colorants from wastewater: A review on sources and treatment strategies. *J. Ind. Eng. Chem.* **2019**, *75*, 1-19, DOI: 10.1016/j.jiec.2019.02.011.
- [3] Ghedjemis, A.; Ayeche, R.; Benouadah, A.; Fenineche, N., A new application of hydroxyapatite extracted from dromedary bone: Adsorptive removal of Congo red from aqueous solution. *Int. J. Appl. Ceram. Technol.* **2021**, *18*, 590-597, DOI: 10.1111/ijac.13677.
- [4] El Kassimi, A.; Achour, Y.; El Himri, M.; Laamari, M. R.; El Haddad, M., Process optimization of high surface area activated carbon prepared from Cucumis melo by H₃PO₄ activation for the removal of cationic and anionic dyes using full factorial design. *biointerface. Res. Appl. Chem.* **2021**, *11*, 12662-12679, DOI: 10.33263/BRIAC115.1266212679.
- [5] Achour, Y.; Bahsis, L.; Ablouh, E. H.; Yazid, H.;

- Laamari, M. R.; El Haddad, M., Insight into adsorption mechanism of congo red dye onto bombax buonopozense bark activated-carbon using Central composite design and DFT studies. *Surf. Interfaces*. **2021**, *23*, 100977, DOI: 10.1016/j.surfin.2021.100977.
- [6] Rosenkranz, H. S.; Cunningham, S. L.; Mermelstein, R.; Cunningham, A. R., The challenge of testing chemicals for potential carcinogenicity using multiple shortterm assays: an analysis of a proposed test battery for hair dyes. *Mut. Res. Genetic. Toxicol. Environ. Mutagenesis*. **2007**, *633*, 55-66, DOI: 10.1016/j.mrgentox.2007.05.008.
- [7] Jawad, A. H.; Abdulhameed, A. S., Mesoporous Iraqi red kaolin clay as an efficient adsorbent for methylene blue dye: Adsorption kinetic, isotherm and mechanism study. *Surf. Interfaces*. **2020**, *18*, 100422, DOI: 10.1016/j.surfin.2019.100422.
- [8] Abbas, M., Experimental investigation of titanium dioxide as an adsorbent for removal of Congo red from aqueous solution, equilibrium and kinetics modeling. *J. Water. Reuse. Desal.* **2020**, *10*, 251-266, DOI: 10.2166/wrd.2020.038.
- [9] Karatas, M.; Argun, Y. A.; Argun, M. E., Decolorization of antraquinonic dye, Reactive blue 114 from synthetic wastewater by fenton process: kinetics and thermodynamics. *J. Ind. Eng. Chem.* **2012**, *18*, 1058-1062, DOI: 10.1016/j.jiec.2011.12.007.
- [10] Virk, A. K.; Thakur, P.; Sharma, I.; Swati, Kumari, C.; Chauhan, A.; Li, X.; Salama, E. -S.; Kulshrestha, S., A moringa oleifera seeds-based filter for efficient removal of congo red from aqueous medium. *Desalination. Water. Treat.* **2020**, *206*, 371-384, DOI: 10.5004/dwt.2020.26251.
- [11] Moussavi, G.; Mahmoudi, M., Degradation and biodegradability improvement of the reactive red 198 azo dye using catalytic ozonation with MgO nanocrystals. *Chem. Eng. J.* **2009**, *152*, 1-7, DOI: 10.1016/j.cej.2009.03.014.
- [12] Essadki, A. H.; Bennajah, M.; Gourich, B.; Vial, C. H.; Azzi, M.; Delmas, H., Electrocoagulation/electroflotation in an external-loop airlift reactor- Application to the decolorization of textile dye wastewater: a case study. *Chem. Eng. Process.* **2008**, *47*, 1211-1223, DOI: 10.1016/j.cep.2007.03.013.
- [13] Wang, A.; Qu, J.; Liu, H.; Ge, J., Degradation of azo dye Acid Red 14 in aqueous solution by electrokinetic and electrooxidation process. *Chemosphere*. **2004**, *55*, 1189-1196, DOI: 10.1016/j.chemosphere.2004.01.024.
- [14] Alventosa-deLara, E.; Barredo-Damas, S.; Alcaina-Miranda, M. I.; Iborra-Clar, M. I., Ultrafiltration technology with a ceramic membrane for reactive dye removal: Optimization of membrane performance. *J. Hazard. Mater.* **2012**, *209-210*, 492-500, DOI: 10.1016/j.jhazmat.2012.01.065.
- [15] Paul, J.; Rawat, K. P.; Sarma, K. S. S.; Sabharwal, S., Decoloration and degradation of Reactive Red-120 dye by electron beam irradiation in aqueous solution. *Appl. Rad. Isotopes*. **2011**, *69*, 982-987, DOI: 10.1016/j.apradiso.2011.03.009.
- [16] Koparal, A. S.; Yavuz, Y.; Gurel, C.; Ogutveren, U. B., Electrochemical degradation and toxicity reduction of C.I. Basic Red 29 solution and textile wastewater by using diamond anode. *J. Hazard. Mater.* **2007**, *145*, 100-108, DOI: 10.1016/j.jhazmat.2006.10.090.
- [17] Liua, C. H.; Wua, J. S.; Chiua, H. C.; Suena, S. Y.; Chub, K. H., Removal of anionic reactive dyes from water using anion exchange membranes as adsorbers. *Water. Res.* **2007**, *41*, 1491-1500, DOI: 10.1016/j.watres.2007.01.023.
- [18] Sudarjanto, G.; Lehmann, B. K.; Keller, J., Optimization of integrated chemical-biological degradation of a reactive azo dye using response surface methodology. *J. Hazard. Mater.* **2006**, *138*, 160-168, DOI: 10.1016/j.jhazmat.2006.05.054.
- [19] Cardoso, N. F.; Lima, E. C.; Pinto, I. S.; Amavisca, C. V.; Royer, B.; Pinto, R. B.; Alencar, W. S.; Pereira, S. F. P., Application of cupuassu shell as biosorbent for the removal of textile dyes from aqueous solution. *J. Environ. Manag.* **2011**, *92*, 1237-1247, DOI: 10.1016/j.jenvman.2010.12.010.
- [20] El Kassimi, A.; Achour, Y.; El Himri, M.; Laamari, R.; El Haddad, M., Removal of two cationic dyes from aqueous solutions by adsorption onto local clay: experimental and theoretical study using DFT method.

- Int. J. Environ. Anal. Chem.* **2021**, 1-22, DOI: 10.1080/03067319.2021.1873306.
- [21] El Kassimi, A.; Boutouil, A.; El Himri, M.; Rachid Laamari, M.; El Haddad, M., Selective and competitive removal of three basic dyes from single, binary and ternary systems in aqueous solutions: A combined experimental and theoretical study. *J. Saudi. Chem. Soc.* **2020**, *24*, 527-544, DOI: 10.1016/j.jscs.2020.05.005.
- [22] El Haddad, M.; Mamouni, R.; Saffaj, N.; Lazar, S., Removal of a cationic dye-basic red 12- from aqueous solution by adsorption onto animal bone meal. *J. Assoc. Arab. Univ. Basic. Appl. Sci.* **2012**, *12*, 48-54, DOI: 10.1016/j.jaubas.2012.04.003.
- [23] El Haddad, M.; Regti, A.; Slimani, R.; Lazar, S., Assessment of the biosorption kinetic and thermodynamic for the removal of safranin dye from aqueous solutions using calcined mussel shells. *J. Ind. Eng. Chem.* **2014**, *20*, 717-724, DOI: 10.1016/j.jiec.2013.05.038.
- [24] El Kassimi, A.; Achour, Y.; El Himri, M.; Laamari, R.; El Haddad, M., High efficiency of natural safiot clay to remove industrial dyes from aqueous media: kinetic, isotherm adsorption and thermodynamic studies. *Biointerface. Res. Appl. Chem.* **2021**, *11*, 12717-12731, DOI: 10.33263/BRIAC115.1271712731.
- [25] Mahmoodi, N. M.; Hayati, B.; Arami, M.; Lan, C., Adsorption of textile dyes on pine cone from colored wastewater: Kinetic, equilibrium and thermodynamic studies. *Desalination.* **2011**, *268*, 117-125, DOI: 10.1016/j.desal.2010.10.007.
- [26] Reddy, M. C. S.; Sivaramakrishna, L.; Reddy, A. V., The use of an agricultural waste material, Jujuba seeds for the removal of anionic dye (Congo red) from aqueous medium. *J. Hazard. Mater.* **2012**, 203-204, 118-127, DOI: 10.1016/j.jhazmat.2011.11.083.
- [27] Arab, C.; El Kurdi, R.; Patra, D., Efficient removal of Congo red using curcumin conjugated zinc oxide nanoparticles as new adsorbent complex. *Chemosphere.* **2021**, *276*, 130158, DOI: 10.1016/j.chemosphere.2021.130158.
- [28] El Kassimi, A.; Regti, A.; Laamari, M. R.; El Haddad, M., Assessment and enhancement of powdered and activated carbon derived from persea nuts for adsorptive removal dyes from wastewaters. *Der. Pharma. Chem.* **2017**, *9*, 38-45.
- [29] Bulut, E.; Ozacar, M.; Sengil, I. A., Equilibrium and kinetic data and process design for adsorption of congo red onto bentonite. *J. Hazard. Mater.* **2008**, *154*, 613-622, DOI: 10.1016/j.jhazmat.2007.10.071.
- [30] Low, B. T.; Ting, Y. P.; Deng, S., Surface modification of Penicillium chrysogenum mycelium for enhanced anionic dye removal. *Chem. Eng. J.* **2008**, *141*, 9-17, DOI: 10.1016/j.cej.2007.10.004.
- [31] Wang, B. E.; Hu, Y. Y.; Xie, L.; Peng, K., Biosorption behavior of azo dye by inactive CMC immobilized Aspergillus fumigatus beads. *Bioresour. Technol.* **2008**, *99*, 794-800, DOI: 10.1016/j.biortech.2007.01.043.
- [32] Lagergren, S., Zur theorie der sogenannten adsorption gelöster stoffe, *Kunliga Svenska, Vetenskapsakademiens. Handlingar.* 1898, *24*, 1-39.
- [33] Ho, Y. S.; McKay, G., Pseudo-second-order model for sorption processes. *Process. Biochem.* **1999**, *34*, 451-465, DOI: 10.1016/S0032-9592(98)00112-5.
- [34] Xiong, X. J.; Meng, X. J.; Zheng, T. L., Biosorption of C.I. Direct blue 199 from aqueous solution by nonviable aspergillus niger. *J. Hazard. Mater.* **2010**, *175*, 241-6, DOI: 10.1016/j.jhazmat.2009.09.155.
- [35] Achour, Y.; Khouili, M.; Abderrafia, H.; Melliani, S.; Laamari, M. R.; El Haddad, M., DFT investigations and experimental studies for competitive and adsorptive removal of two cationic dyes onto an eco-friendly material from aqueous media. *Int. J. Environ. Res.* **2018**, *12*, 789-802, DOI: 10.1007/s41742-018-0131-x.
- [36] Langmuir, I., The adsorption of gases on plane surfaces of glass, mica and platinum. *J. Am. Chem. Soc.* **1916**, *40*, 1361-1403.
- [37] Freundlich, H. M., Über die adsorption in losungen. *Z. Phys. Chem.* 1906, *57*, 385-470.
- [38] El Kassimi, A.; Achour, Y.; El Himri, M.; Laamari, M. R.; El Haddad, M., Optimization of preparation conditions of highly efficient activated carbon for use in water treatment-experimental design approach. *Int. J. Environ. Anal. Chem.*, **2021**, 1-23, DOI: 10.1080/03067319.2020.1861261.